Dynamical Structure Factor of the Homogeneous Electron Liquid: Its Accurate Shape and the Interpretation of Experiments on Aluminum

Yasutami Takada[1] and Hiroshi Yasuhara[2]

[1]*Institute for Solid State Physics, University of Tokyo, Kashiwa, Chiba 277-8581, Japan*
[2]*Department of Physics, Graduate School of Science, Tohoku University, Sendai 980-8578, Japan*

(Received 27 December 2001; published 1 November 2002)

Based on a highly self-consistent theory maintaining the exact functional relations between the self-energy and the vertex part, we evaluate the dynamical structure factor $S(\mathbf{q}, \omega)$ of the electron liquid. We find striking deviations from $S(\mathbf{q}, \omega)$ in the random-phase approximation (RPA) for $|\mathbf{q}| > p_F$; besides a broad peak in the one-pair excitation region as seen in the RPA, a clear shoulder appears along a steepened slope at low ω due to electron-hole multiple scattering, and a flattened structure follows due to inseparable interference between one-pair and multipair excitations. Our result agrees with experiments on Al on the whole. The remaining discrepancy is ascribed to the band-structure-induced effect.

DOI: 10.1103/PhysRevLett.89.216402 PACS numbers: 71.10.Ca, 71.35.–y, 71.45.Gm, 78.20.Bh

The electron liquid, an assembly of N electrons embedded in a uniform positive background, has been studied to clarify the nature of electron correlation in metals, putting aside the influence of the periodic ion potential. This simplified model poses a tough problem, but after the struggles lasting longer than half a century [1], accurate knowledge of its almost all static properties is now acquired by a number of sophisticated methods including quantum Monte Carlo (QMC) simulations [2,3] over the entire region of metallic densities $1.88 < r_s < 5.6$, where r_s is the conventional density parameter.

As for dynamical properties, on the other hand, our knowledge is still not enough in spite of all previous efforts [4–8] to go beyond the random-phase approximation (RPA) in an attempt to explain the double-peak structure in the dynamical structure factor $S(\mathbf{q}, \omega)$ observed in light metals such as Al [9–11]. Among approximation schemes, the Baym-Kadanoff conserving one [12] formulated in terms of the full Green's function G is most suitable for the evaluation of $S(\mathbf{q}, \omega)$. Accuracy of the result depends critically on the choice of the energy functional $\Phi[G]$, but the result will never become exact, since no algorithm is known to give the exact $\Phi[G]$.

One of the authors (Y.T.) developed a conceptually different scheme to obtain the exact $S(\mathbf{q}, \omega)$ [13]; instead of pursuing $\Phi[G]$, we pay attention to the exact functional relations between the self-energy Σ and the vertex function Γ, obeying the microscopic conservation law. In particular, Γ is determined by the Bethe-Salpeter equation with an irreducible electron-hole interaction given by the functional derivative, $\delta\Sigma/\delta G$. Starting from an arbitrary input, we iteratively revise both Σ and Γ simultaneously towards self-consistency through the relations, whereby the number of terms representing Σ generated in this iterative process rapidly increases, eventually covering all terms derivable from the exact $\Phi[G]$ when the self-consistency is achieved. In a numerical algorithm, however, the functional differentiation $\delta\Sigma/\delta G$ is not feasible. Thus, we need to invent an alternative scheme to revise Γ on a computer in an accurate and efficient way.

Recently, a physically motivated and accurate enough prescription is given for Γ [14]. In this Letter, our result of $S(\mathbf{q}, \omega)$ is presented, which is most accurate among all existing results. Striking differences can be seen between our result and the RPA one, particularly for $|\mathbf{q}|$ larger than p_F the Fermi momentum. Our result describes inseparable coupling between one-pair and multipair excitations in the one-pair excitation region, attractive electron-hole multiple scattering (excitonic effect) on the low-ω side of the one-pair region, and extra contributions from multipair excitations outside of it. By comparing it with the experimental $S(\mathbf{q}, \omega)$ on Al, we conclude that Al can be regarded as the electron liquid for ω smaller than about the Fermi energy $E_F(\approx 11$ eV). For larger ω, we must allow for the strong tight-binding nature of unoccupied $3d$ and $4f$ bands in analyzing experiments.

At temperature T, $S(\mathbf{q}, \omega)$ is written as [15]

$$S(\mathbf{q}, \omega) = -\frac{1}{\pi}\frac{1}{1 - e^{-\omega/T}}\,\mathrm{Im}\, Q_c(\mathbf{q}, \omega), \tag{1}$$

where $Q_c(\mathbf{q}, \omega)$ is the density-density correlation function, given in terms of $\Pi(\mathbf{q}, \omega)$ the polarization function as $Q_c(\mathbf{q}, \omega) = -\Pi(\mathbf{q}, \omega)/[1 + V(\mathbf{q})\Pi(\mathbf{q}, \omega)]$ with the Coulomb interaction $V(\mathbf{q}) = 4\pi e^2/\mathbf{q}^2$. We shall obtain $\Pi(\mathbf{q}, \omega)$ by analytic continuation of $\Pi(\mathbf{q}, i\omega_l)$ onto the real ω axis, where ω_l is a boson Matsubara frequency, expressed as $i\omega_l \equiv 2\pi i T l$ with an integer l.

In order to determine $\Pi(q)$ with $q \equiv (\mathbf{q}, i\omega_l)$, we need to implement the following self-consistent loop to relate $\Pi(q)$ with $\Sigma(p)$ the electron self-energy, where p is a combined notation of momentum $\mathbf{p}$ and fermion Matsubara frequency $i\omega_n \equiv \pi i T(2n + 1)$ with an integer n:

$$\Sigma(p) = -T\sum_{\omega_l}\sum_{\mathbf{q}} V(\mathbf{q})G(p+q)\Gamma(p,p+q)/\varepsilon(q), \tag{2}$$

where $G(p)$ is given by $G(p)^{-1} = G^{(0)}(p)^{-1} - \Sigma(p)$ with $G^{(0)}(p)^{-1} = i\omega_n - \epsilon_{\mathbf{p}}$ using $\epsilon_{\mathbf{p}}$ the bare one-electron dispersion, $\varepsilon(q)$ is the dielectric function, defined by $\varepsilon(q) \equiv 1 + V(\mathbf{q})\Pi(q)$ with $\Pi(q)$, calculated as

$$\Pi(q) = -T\sum_{\omega_n}\sum_{\mathbf{p}\sigma} G(p)G(p+q)\Gamma(p,p+q). \tag{3}$$

The crux in these equations is $\Gamma(p, p+q)$ for which an effective scheme is invented [14] to give $\Gamma(p, p+q)$ as the product of two factors, $\Gamma_{\mathrm{LFC}}(q) \equiv 1 - f_{\mathrm{xc}}^{\mathrm{hom}}(q)\Pi(q)$ and $\Gamma_{\mathrm{WI}}(p, p+q) \equiv [G(p)^{-1} - G(p+q)^{-1}]/[G^{(0)}(p)^{-1} - G^{(0)}(p+q)^{-1}]$, where $f_{\mathrm{xc}}^{\mathrm{hom}}(q)$ is the frequency-dependent exchange-correlation local-field correction appearing in the time-dependent density functional theory [16]. Irrespective of the choice of $f_{\mathrm{xc}}^{\mathrm{hom}}(q)$, Γ_{WI} enforces the Ward identity (WI). Using $\Gamma = \Gamma_{\mathrm{LFC}}\Gamma_{\mathrm{WI}}$, we can implement the self-consistent iteration loop, starting from the noninteracting solution and ending the loop if the relative difference in $\Sigma(p)$ between input and output becomes less than 10^{-5} for any p.

Calculations are done for the electron liquid with the parabolic dispersion $\epsilon_{\mathbf{p}} = \mathbf{p}^2/2m$ for $1 \le r_s \le 5$. We have set T at $0.01E_{\mathrm{F}}$ which is low enough to obtain $Q_c(\mathbf{q}, \omega)$ or $S(\mathbf{q}, \omega)$ at $T = 0$ by analytic continuation of $\Pi(\mathbf{q}, i\omega_l)$ onto the real ω axis. In the inset of Fig. 1, we have compared our result of $Q_c(\mathbf{q}, 0)$ with the virtually exact one in the QMC [3], showing that our result of $\Pi(\mathbf{q}, 0)$ calculated through Eq. (3), is very accurate for any $\mathbf{q}$. This assures the overall accuracy of the summed quantities in Eq. (3), G and Γ, eventually confirming the correctness and good self-consistency of our theory.

Throughout the metallic-density region, qualitative features of $S(\mathbf{q}, \omega)$ remain the same; a typical example at $r_s = 5$ is given in Fig. 1. For $|\mathbf{q}| < q_c$ ($\approx 0.90p_{\mathrm{F}}$), $S(\mathbf{q}, \omega)$ is characterized by a single peak at $\omega = \omega_p(q)$, the plasmon. Both its dispersion $\omega_p(q)$ and its cutoff momentum q_c are slightly lower than those of the RPA; q_c in the RPA is $1.1p_{\mathrm{F}}$. Even if $|\mathbf{q}|$ is not very close to q_c, this peak has a rather broad damping width in contrast with an undamped peak of the RPA. This damping comes from coupling between the plasmon and multipair excitations. As seen in Fig. 2(d), the plasmon is no longer well defined beyond q_c because of the Landau damping inside the one-pair excitation region. Incidentally, it is a rather astonishing fact that the bulk of $S(\mathbf{q}, \omega)$ occupies almost the same region as the noninteracting one-pair region, though a considerable amount of damping widths associate with the quasiparticles; minor contributions from multipair excitations are seen outside the one-pair region. Here we note that this fact, though being physically natural, cannot be obtained without Γ_{WI}.

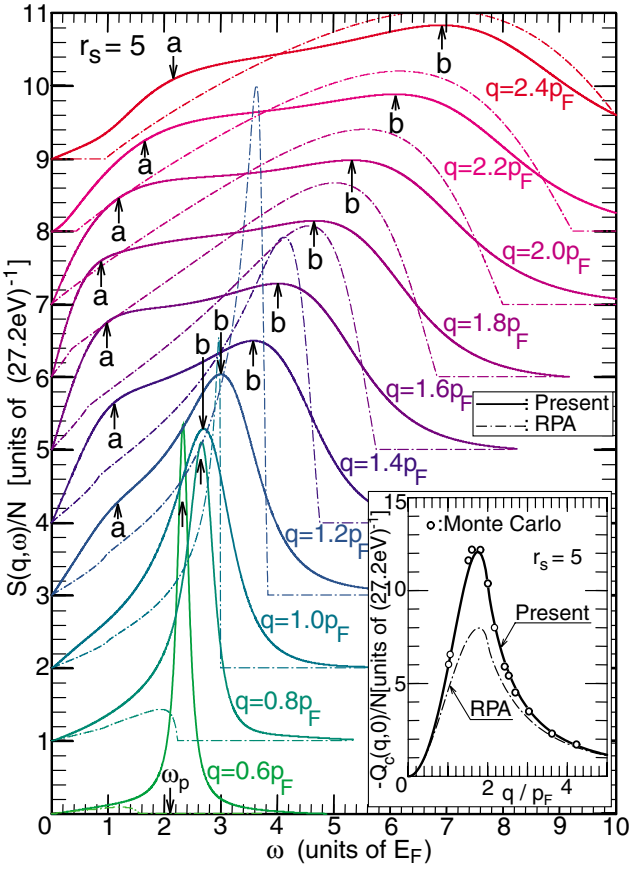

FIG. 1 (color online). Dynamical structure factor of the electron liquid at $r_s = 5$. In the inset, the obtained static density-density correlation function is compared with that in the QMC [3]. The value indicated by ω_p is the plasmon energy at $\mathbf{q} = 0$.

A novel structure is found in $S(\mathbf{q}, \omega)$ for $|\mathbf{q}| > q_c$ or p_{F}; besides a broad peak b located at almost the same position in the RPA, there appears a clear shoulder a accompanied by a steepened slope of the linear term in $S(\mathbf{q}, \omega)$ for small ω. The peak b, being identified as "the center of gravity" of one-pair excitations, is transformed continuously into the plasmon peak as $|\mathbf{q}|$ decreases. The shoulder a is well developed particularly for $1.4 \le |\mathbf{q}|/p_{\mathrm{F}} \le 2$ and the slope is surprisingly enhanced over the RPA value accordingly. Even for $|\mathbf{q}| > 2p_{\mathrm{F}}$, where $S(\mathbf{q}, \omega)$ varies in proportion to ω^3 for small ω due to two-pair excitations, the shoulder a is still perceptible at ω, well above the threshold of the one-pair region [$\approx (\mathbf{q}^2 - 2p_{\mathrm{F}}|\mathbf{q}|)/2m$], giving a large enhancement of $S(\mathbf{q}, \omega)$. Around the threshold, one-pair and multipair excitations are superimposed and inseparably interfere.

The same interference effect is considered to bring about the flattened structure of $S(\mathbf{q}, \omega)$ seen between a and b for $|\mathbf{q}| \ge 1.4p_{\mathrm{F}}$. In fact, the lowest-order term in perturbation for the two-pair contribution to $S(\mathbf{q}, \omega)$ diverges in the one-pair region, because the self-energy-insertion term includes the energy denominator squared

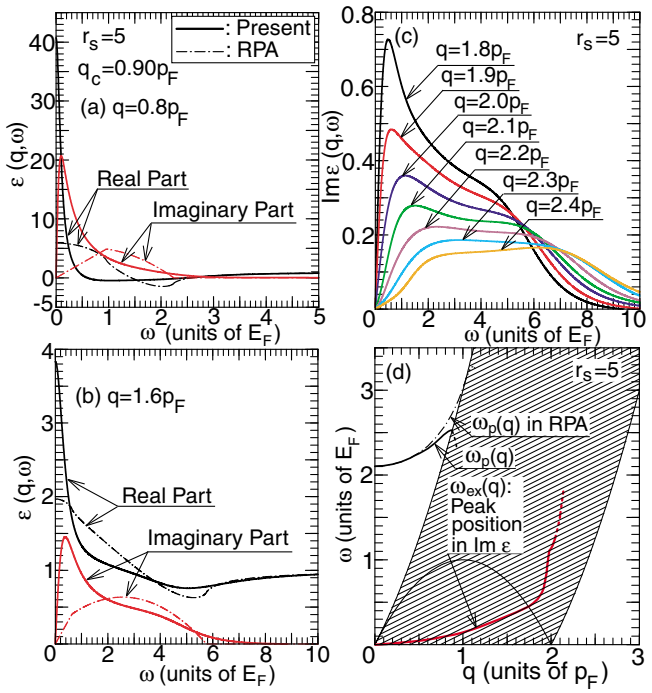

FIG. 2 (color online). Dielectric function at (a) $q = 0.8p_F$ and (b) $q = 1.6p_F$ compared with that in the RPA for the electron liquid at $r_s = 5$. Its imaginary part is given for q in the range $(1.8–2.4)p_F$ in (c), while in (d) the peak position in $\mathrm{Im}\,\varepsilon(\mathbf{q}, \omega)$, $\omega_{ex}(q)$ is plotted in the (q, ω) plane, together with the plasmon dispersion $\omega_p(q)$ determined by the zeros of $\mathrm{Re}\,\varepsilon(\mathbf{q}, \omega)$ in both the present method and the RPA. The hatched area represents the one-pair excitation region drawn using the bare dispersion $\epsilon_{\mathbf{p}}$.

which vanishes at the same time as the very argument in the energy-conserving δ function. Even stronger divergences occur in higher-order terms due to repeated self-energy insertions, piling up the same energy denominators; the same applies to multipair contributions. These divergent terms can be tamed into the convergent $S(\mathbf{q}, \omega)$ by taking an infinite sum using G, not $G^{(0)}$, which makes one-pair and multipair excitations inseparable [5].

To trace the origin of a, we plot $\varepsilon(\mathbf{q}, \omega)$ in Fig. 2 at various values of $|\mathbf{q}|$. The present dielectric function deviates drastically from the RPA result; the most salient feature is the presence of a sharp peak in $\mathrm{Im}\,\varepsilon(\mathbf{q}, \omega)$ at low ω, representing a drastic lower shift of one-pair excitation energies from those in the RPA. In Fig. 2(d), the peak position in $\mathrm{Im}\,\varepsilon(\mathbf{q}, \omega)$, $\omega_{ex}(q)$, is plotted; it stays in the one-pair region and increases almost linearly with q for small q, but it rises abruptly near the internal boundary of the one-pair region, $\omega = (2p_F q - q^2)/2m$, followed by a small anomaly at $q \approx 2p_F$. Thereafter, as seen in Fig. 2(c), the peak gradually disappears. This sharp peak in $\mathrm{Im}\,\varepsilon(\mathbf{q}, \omega)$ gives rise to the shoulder a of $S(\mathbf{q}, \omega)$, though the peak position is not the same as a, since $S(\mathbf{q}, \omega)$ is not directly related to $\mathrm{Im}\,\varepsilon(\mathbf{q}, \omega)$ but to $\mathrm{Im}\,\varepsilon(\mathbf{q}, \omega)/|\varepsilon(\mathbf{q}, \omega)|^2$. For $q < q_c$ or p_F, the shoulder a disappears due to the huge value of $\mathrm{Re}\,\varepsilon(\mathbf{q}, \omega)$.

The sharp peak above may be ascribed to the electron-hole multiple scattering. The RPA describes an independent electron-hole pair, giving the excitation energy as $|\epsilon_{\mathbf{p}+\mathbf{q}} - \epsilon_{\mathbf{p}}|$, but actually the attractive screened potential works between the pair; this attraction effectively reduces the excitation energy. The sharp peak is then interpreted as an excitonic effect [17]. The possibility of this effect to enhance the interband optical conductivity of sodium was suggested by a simple model calculation [18].

Now we consider $S(\mathbf{q}, \omega)$ of Al, a metal regarded as most electron-liquid-like with $r_s = 2.08$. Inelastic x-ray scattering experiments give a well-converged $S(\mathbf{q}, \omega)$ [9–11]; a complex structure composed of $\mathbf{q}$-orientation-independent double peaks for large $|\mathbf{q}|$ is confirmed. Such a complex structure has been attributed mainly to the band-structure effect [19,20] by comparing the experiment with $S_{\mathrm{band}}(\mathbf{q}, \omega)$ the Lindhard-like dynamical structure factor calculated with the Bloch functions given in the LDA (local-density approximation). To improve on the theory, effects of exchange and correlation should be included in $S_{\mathrm{band}}(\mathbf{q}, \omega)$. The effects have long been treated in terms of the local-field correction, which amounts to approximating $\Gamma(p, p + q)$ simply to $\Gamma_{\mathrm{LFC}}(q)$ with $f_{\mathrm{xc}}^{\mathrm{hom}}(q)$ chosen to reproduce the experiment. This is called the time-dependent-LDA approach [11,21].

We shall make a different approach to the experimental $S(\mathbf{q}, \omega)$, since accurate knowledge of $S(\mathbf{q}, \omega)$ of the electron liquid is now available; we first compare theory with experiment without any adjustable parameters and then

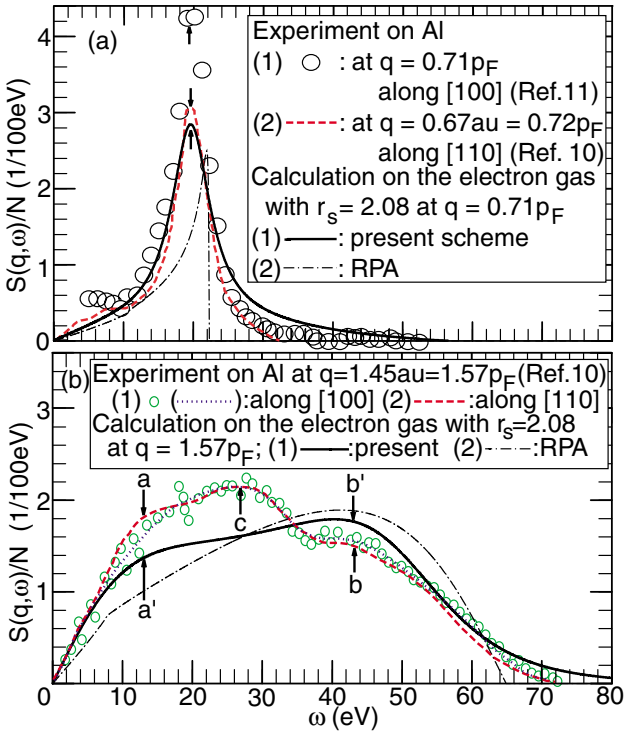

FIG. 3 (color online). Comparison between $S(\mathbf{q}, \omega)$ of the electron liquid at $r_s = 2.08$ and the experimental one for Al metal.

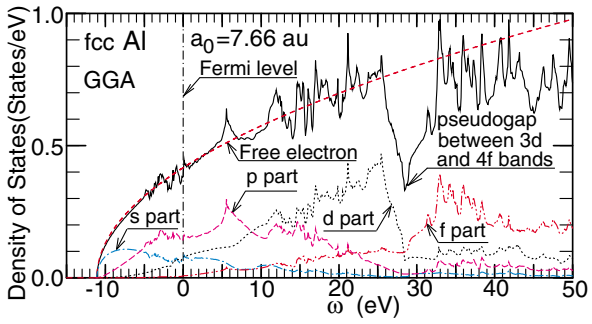

FIG. 4 (color online). Density of states, both total and partial wave, for fcc Al calculated in the GGA using the package WIEN97.

identify the band-structure-induced effect. In Fig. 3, two typical cases are shown for comparison; (a) shows the plasmon-dominant region ($q < q_c$ with $q_c \approx 0.8 p_F$), and (b) shows the one-shoulder-one-peak region ($q \gtrsim 1.4 p_F$). In (a), we find that the electron-liquid model reproduces very well the peak position of the plasmon and its damping width; besides the plasmon peak, a few **q**-orientation-dependent small structures are experimentally observed, but they are ascribed to the band-structure effects such as the so-called zone-boundary collective states [10,21,22].

In (b), significant differences can be seen between theory and experiment, but a closer inspection reveals a few important points: (i) For $\omega < E_F (\approx 11$ eV), a quite good agreement can be seen, irrespective of **q**, indicating the relevance of the electron-liquid model to Al. (ii) In Fig. 3(b), a reasonable correspondence can be seen between two characteristic energies of theory, a' and b', and those in experiment, a and b, respectively; this implies that some characteristic features of the electron liquid persist in Al even for $\omega > E_F$. (iii) The present theory gives no peak at c. Thus, the peak c should be attributed to the band-structure effect in line with the analysis with the use of $S_{\text{band}}(\mathbf{q}, \omega)$ [10,20,21], suggesting that this peak reflects the existence of a pseudogap between b and c, namely, around $\omega \approx 30$ eV, as seen in the LDA band calculation [23].

In order to clarify the origin of the pseudogap, we perform a band-structure calculation of fcc Al using the GGA (generalized gradient expansion approximation) [24] and analyze the density of states (DOS) into partial-wave components, as seen in Fig. 4. We make some observations: (i) Very good agreement is obtained between the total DOS of the band calculation and that of the free-electron model for $\omega < 5$ eV and reasonably good agreement for $\omega < 25$ eV above the Fermi level. (ii) A large pseudogap is seen around 30 eV, invalidating the application of the electron-liquid model to Al in this energy region or above. (iii) The partial-wave analysis reveals that the pseudogap is created by two factors: (1) the narrowness of both $3d$ and $4f$ bands and (2) a large enough separation between those bands. We also ascertain that such a pseudogap cannot be seen in Na by performing a similar calculation. Hence, the appearance of such a pseudogap depends entirely on the difference in the strength of the ionic potentials between Al^{3+} and Na^{+}. We may thus conclude that the peak c reflects the strong tightly binding nature of unoccupied $3d$ and $4f$ bands in Al. It is interesting that nearly localized states exist well above the extended $3s$ and $3p$ bands.

In summary, we have given an accurate calculation of $S(\mathbf{q}, \omega)$ of the electron liquid and discussed its characteristic features and their physical meanings. We have analyzed the experiments on Al and found that the electron-liquid model applies to Al on the whole and especially well for $\omega < E_F$. The discrepancy from the model may be mainly ascribed to the strong tight-binding nature of unoccupied $3d$ and $4f$ bands in Al.

[1] L. Hedin, Phys. Rev. **139**, A796 (1965); L. Hedin and S. Lundqvist, in *Solid State Physics*, edited by F. Seitz *et al.* (Academic, New York, 1969), Vol. 23, p. 1.
[2] D. M. Ceperley and B. J. Alder, Phys. Rev. Lett. **45**, 566 (1980).
[3] S. Moroni *et al.*, Phys. Rev. Lett. **75**, 689 (1995).
[4] G. Mukhopadhyay *et al.*, Phys. Rev. Lett. **34**, 950 (1975).
[5] K. Awa *et al.*, Phys. Rev. B **25**, 3670 (1982).
[6] S. Rahman and G. Vignale, Phys. Rev. B **30**, 6951 (1984).
[7] T. K. Ng and B. Dabrowski, Phys. Rev. B **33**, 5358 (1986).
[8] F. Green *et al.*, Phys. Rev. B **31**, 2779 (1985); **31**, 2796 (1985); **31**, 5837 (1985); **35**, 124 (1987).
[9] P. M. Platzman and P. Eisenberger, Phys. Rev. Lett. **33**, 152 (1974); P. M. Platzman *et al.*, Phys. Rev. B **46**, 12 943 (1992).
[10] W. Schülke *et al.*, Phys. Rev. B **47**, 12 426 (1993).
[11] B. C. Larson *et al.*, Phys. Rev. Lett. **77**, 1346 (1996).
[12] G. Baym and L. P. Kadanoff, Phys. Rev. **124**, 287 (1961); G. Baym, Phys. Rev. **127**, 1391 (1962).
[13] Y. Takada, Phys. Rev. B **52**, 12 708 (1995).
[14] Y. Takada, Phys. Rev. Lett. **87**, 226402 (2001).
[15] We employ units in which $\hbar = k_B = 1$.
[16] E. K. U. Gross *et al.*, in *Density Functional Theory II*, edited by R. F. Nalewajski (Springer-Verlag, Berlin, 1996), Chap. 2, p. 81.
[17] The excitonic effect is discussed in real solids in the electron-hole ladder approximation: W. Hanke and L. J. Sham, Phys. Rev. B **21**, 4656 (1980); S. Albrecht *et al.*, Phys. Rev. Lett. **80**, 4510 (1998); L. X. Benedict *et al.*, Phys. Rev. Lett. **80**, 4514 (1998).
[18] M. Higuchi and H. Yasuhara, J. Phys. Soc. Jpn. **69**, 2099 (2000).
[19] N. E. Maddocks *et al.*, Europhys. Lett. **27**, 681 (1994).
[20] A. Fleszar *et al.*, Phys. Rev. Lett. **74**, 590 (1995).
[21] B. C. Larson *et al.*, J. Phys. Chem. Solids **61**, 391 (2000).
[22] E-Ni Foo and J. J. Hopfield, Phys. Rev. **173**, 635 (1968); K. Sturm and L. E. Oliveira, Phys. Rev. B **30**, 4351 (1984).
[23] J. W. D. Connolly, Int. J. Quantum Chem. **3S**, 807 (1970); E. Ojala, Phys. Status Solidi (b) **119**, 269 (1983).
[24] P. Blaha, K. Schwarz, and J. Luitz, WIEN97, Vienna University of Technology, Vienna, 1997.